

Short Communication

Effect of Technological Parameters on the Electrowinning of Cobalt from Cobalt(II) Chloride Solutions

Rudi Subagja*, Iwan Setiawan, Ahmad Rizky Rhamdani, and Januar Irawan

Research Center for Metallurgy, National Innovation Research Agency, Indonesia

*E-mail: rudi001@brin.go.id; rudibagja003@gmail.com

Received: 3 June 2022/Accepted: 20 July 2022/Published: 7 August 2022

The effect of technological parameters such as current density, temperature, cobalt concentration, and pH of electrolyte solutions on current efficiency and cobalt morphology during the electrowinning of cobalt from a cobalt chloride solution was observed in an electrowinning cell with a capacity of 500 mL. The experimental results revealed that the cathode current efficiency increased either when the cobalt concentration in the electrolyte solution was increased from 14 to 70 g/L, when the pH of the electrolyte solutions was increased from 0.5 to 2, or when the electrolyte temperature was increased from 30 °C to 60 °C. However, the cathode current efficiency decreased when the current density was increased from 0.8 to 8 A/dm². The highest current efficiency (96%) was obtained at a current density of 0.8 A/dm² in the electrolyte solution with a cobalt concentration of 70 g/L and at a temperature of 60 °C and a pH of 1.5. The scanning electron microscopy micrographs revealed that the cobalt deposit morphology tended to be homogeneous and more compact at a low current density. However, cobalt deposits with large particle sizes and a tendency to be more porous and incompact were formed in the electrolyte solution with a relatively low cobalt concentration. The cobalt deposit morphology that was formed in the electrolyte solution with a low pH tended to become more porous. Furthermore, when the electrolyte temperature was increased to 60 °C, the cobalt deposit morphology that was formed in electrolyte solutions with a cobalt concentration of 30 g/L changed from a mixed small needle-like and oval shape to a large needle-like shape, whereas the cobalt deposit morphology in electrolyte solutions with a cobalt concentration of 70 g/L changed from a small needle-like shape to a circular and more compact shape.

Keywords: cobalt electrowinning, cobalt chloride, current efficiency, cobalt morphology

1. INTRODUCTION

Cobalt has unique chemical and physical properties. Cobalt and its alloys are widely used in many fields to meet the demand for cobalt in commercial applications such as pigments[1][2], drying agents[3], catalysts for converting syngas into high hydrocarbons, and biomass tar reforming[4][5][6]. In the engineering field, cobalt is used in air gas turbines, nuclear power plants, engine vanes, automotive

engines, valve seats, aerospace fuel nozzles, wear resistance applications such as cutting tools[7][8][9], and magnetic materials[10][11]. Samarium cobalt is a magnetic material that has unique capabilities at elevated temperatures, a high corrosion resistance, and a lower cost than FeNdB magnets[12][13]. Cobalt is also used in biomaterial implants, such as knee implants, elbow implants, dental implant prostheses[14][15][16][17], and cardiovascular implants[18], to replace or repair the function of a degenerated human organ. In the energy sector, cobalt is used in batteries[19] and as a cathode for solid oxide fuel cells[20]. Additional information regarding cobalt applications has been reported in a previous publication[21]. The global production of cobalt is increasing owing to its widespread use, and its consumption has changed significantly[22]. The European Commission's science estimated that the global consumption of cobalt will reach 220,000 tons by 2025 and 390,000 tons by 2030[23].

Cobalt is generally obtained as a by-product of nickel, copper, and zinc extraction processes[24][25][26][27][28][29], and from waste battery materials[30]. In laterite nickel ore processing, cobalt is extracted from nickel matte[31][32] or from the by product of the Caron process or the high-pressure acid leaching (HPAL) process[33]. The extraction of cobalt from the by-products of these processes involves using several process steps, such as leaching, solvent extraction, and electrowinning, to precipitate cobalt from the cobalt electrolyte solution. The quality of cobalt produced via the electrowinning process is affected by several process parameters such as the electrolyte composition[34][35]; electrolyte conductivity[36]; impurities in the electrolyte materials[37] and electrode materials[38][39][40]; overpotential[41]; magnetic field[42]; and additives such as hydrogen peroxide[43], tetra ethyl ammonium bromide[44], boric acid[45], and gas bubble[46]. There are numerous research on the cobalt electrowinning process, but only a few research have focused on the effect of current density, temperature, cobalt concentration, and pH of the electrolyte solutions on both the current efficiency and cobalt morphology during the electrowinning of cobalt from cobalt chloride solutions. Therefore, it is crucial to understand the characteristics of cobalt deposits produced on a cathode surface via the electrowinning process because they determine the cobalt quality.

In this study, a cobalt electrowinning experiment was conducted using cobalt chloride solutions to investigate the effect of current density, cobalt concentration, electrolyte solution pH, and temperature on the current efficiency and cobalt deposit morphology.

2. EXPERIMENTAL

Cobalt chloride hexahydrate ($\text{CoCl}_2 \cdot 6\text{H}_2\text{O}$), hydrochloric acid (HCl), and sodium carbonate were used as raw materials in this cobalt electrowinning experiment. The cobalt chloride electrolyte solution was prepared by dissolving $\text{CoCl}_2 \cdot 6\text{H}_2\text{O}$ in demineralized water, and the pH of the electrolyte solution was controlled by adding either HCl or sodium carbonate solution to the cobalt chloride electrolyte solution.

Figure 1 shows a schematic of the cobalt electrowinning experimental apparatus, which was constructed using a 500 mL cylindrical glass as the electrowinning cell, a ruthenium oxide-coated titanium plate as the anode, stainless steel 316 as the cathode, and a Dekko 3030Q power supply rectifier as a direct current source. Prior to use, the stainless steel cathode was polished with #320 SiC sand paper, washed with water, and cleaned with ethanol. The cathode and anode in the electrowinning cell were

separated by a polyester membrane. The distance between the cathode and anode was 1 cm. A cobalt chloride electrolyte solution was poured into the electrowinning cell to begin the experiment. The electrolyte solution was then heated using a hot plate heater until a predetermined solution temperature was reached. After the desired temperature was reached, both the titanium anode and the stainless steel cathode were immersed in the electrolyte solutions in the electrowinning cell. The rectifier supplied a constant direct current into the electrowinning cell through the titanium and stainless steel 316 electrodes at a specified current density.

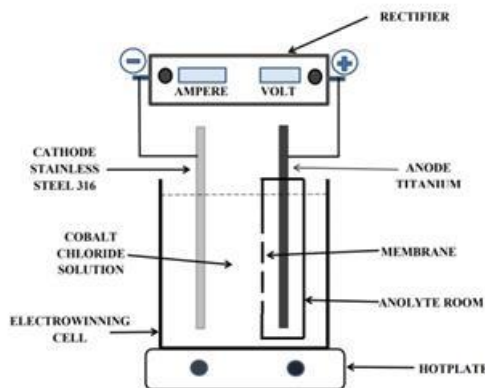


Figure 1. Schematic of the cobalt electrowinning experimental apparatus.

The cobalt electrowinning experiments were conducted for 3 hours using the cobalt chloride electrolyte solution and the following experimental parameters: cobalt concentrations of 14–70 g/L in the electrolyte solution, electrolyte solution pH of 0.5–3, temperatures of 30–60 °C, and applied current densities of 0.8–8 A/dm². After each experiment, both the titanium and stainless steel electrodes were removed from the cell, washed with water, and dried. The cobalt deposits that had formed on the cathode surface were weighed using an analytical balance.

The current efficiency of the cobalt electrowinning process was calculated by comparing the actual mass of cobalt formed on the cathode surface with the theoretical mass of cobalt calculated using equations 1 and 2 according to Faraday’s law. Subsequently, the morphology of the cobalt deposits formed on the cathode surface was observed using scanning electron microscopy (SEM).

$$\text{Current efficiency } E = [(W_A)/(W_T)] \times 100\%, \tag{1}$$

$$W_T = (M_{Co} \times I \times T)/(N F), \tag{2}$$

where E is the current efficiency; W_A is the actual mass of cobalt deposited on the cathode surface; W_T is the theoretical weight of cobalt calculated using Faraday’s law; M_{Co} is the cobalt atomic weight (58.9 g/mol); I is the current (ampere); T is the time (seconds); N is the oxidation state number displaceable electrons per atom; and F is the Faraday constant (96,487 C/mol).

3. RESULTS AND DISCUSSION

3.1. Effect of current density on the current efficiency and cobalt morphology

The effect of current density on the current efficiency was investigated during the electrowinning of cobalt from cobalt chloride solutions with cobalt concentrations of 14–70 g/L at pH 1.5 and a temperature of 60 °C. Current densities of 0.8–8 A/dm² were applied for 3 hours while controlling the amount of current flowing from the rectifier to the cathode and anode in the electrowinning cell.

The cobalt electrowinning experimental results are shown in Figure 2. They demonstrate that the highest current efficiency (96%) was obtained at a current density of 0.8 A/dm² in the electrolyte solution with a cobalt concentration of 70 g/L and at a temperature of 60 °C and a pH of 1.5, increasing the current density from 0.8 to 8 A/dm² decreased the current efficiency for all solutions with different cobalt concentrations. This is because the cobalt deposition process on the cathode surface was faster than the transfer of ionic cobalt from the bulk electrolyte solutions to the cathode surface at relatively high current densities, thereby limiting the rate of cobalt mass transfer through the Nernst diffusion layer and causing more hydrogen evolution to occur since the reduction potential of ionic cobalt is more negative than that of ionic hydrogen[37][47]. The formation of hydrogen gas on the cathode surface decreased the cobalt current efficiency because it used up the current supplied to the electrowinning cell. Another researcher also discovered a similar trend in hydrogen formation during the electrowinning of cobalt from cobalt sulfate solutions[25][53].

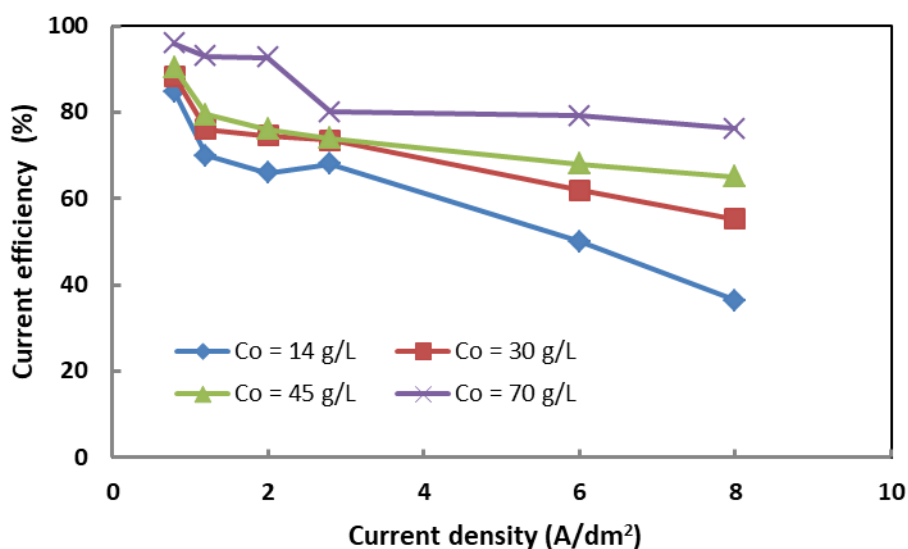


Figure 2. Effect of the current density on the current efficiency at cobalt concentrations of 14–70 g/L, pH 1.5, and a temperature of 60 °C for 3 h.

The formation of hydrogen gas may influence the cobalt morphology formed at the cathode surface. It has been demonstrated that the random formation of hydrogen gas on the electrode surface causes the surface available for cobalt deposition to become rough, resulting in a nonuniform cobalt

deposit morphology[48]. This finding that cobalt deposits tend to become more porous and nonuniform at relatively high current densities is supported by the SEM micrographs of the cobalt deposit morphology shown in Figures 3 and 4. These Figures depict the morphology of the cobalt deposit formed during the electrowinning of cobalt chloride electrolyte solutions with cobalt concentrations of 14 g/L and 70 g/L and electrolyte pH of 1.5 at a temperature of 60 °C and various current densities of 0.8, 1.2, 2, and 2.8 A/dm² for 3 hours.

Figure 3 depicts the needle-like shape of the cobalt particle deposits formed on the cathode surface during the electrowinning of cobalt from the electrolyte solution with a cobalt concentration of 14 g/L. As the current density increased from 0.8 to 2.8 A/dm², the needle-shaped particle size increased, and more porous cobalt deposits were formed on the cathode surface owing to hydrogen formation. Suk discovered a similar result, which demonstrated that high current density resulted in cobalt deposits with large grain sizes and pores during the electrodeposition of cobalt from a cobalt chloride solution[45].

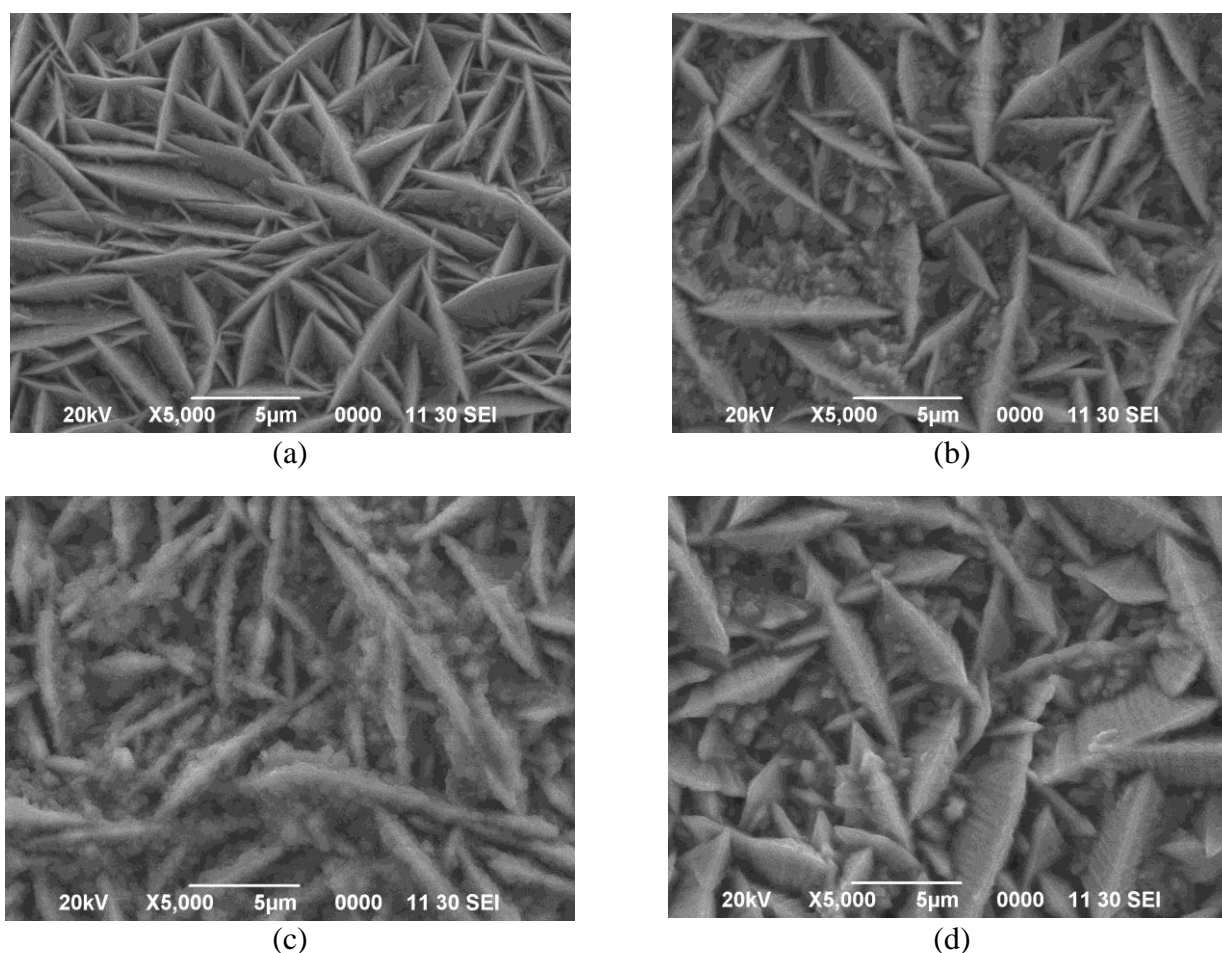


Figure 3. SEM micrograph of the cobalt deposit morphologies formed at a cobalt concentration of 14 g/L, a pH of 1.5, a temperature of 60 °C, and current densities of (a) 0.8 A/dm², (b) 1.2 A/dm², (c) 2 A/dm², and (d) 2.8 A/dm² for 3 h.

Figure 4 shows that the electrowinning of cobalt from electrolyte solutions with a cobalt concentration of 70 g/L resulted in smaller, denser, and less porous cobalt deposits on the cathode

surface, whereas the electrowinning of cobalt from electrolyte solutions with a cobalt concentration of 14 g/L (Figure 3) resulted in more porous and less compact cobalt deposits on the cathode surface.

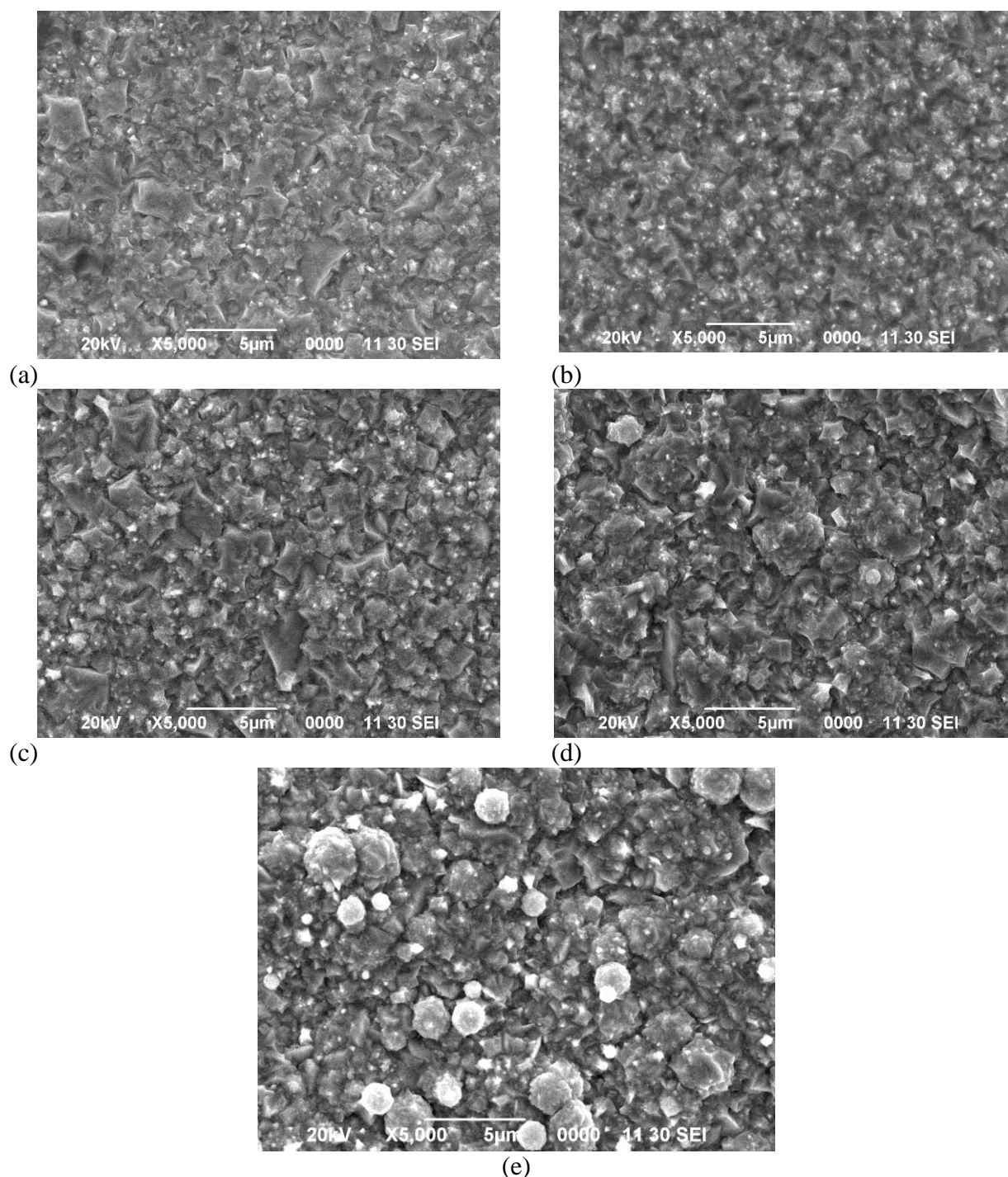


Figure 4. SEM micrograph of the cobalt deposit morphologies formed during electrowinning at a cobalt concentration of 70 g/L, a pH of 1.5, a temperature of 60 °C, and current densities of (a) 0.8 A/dm², (b) 1.2 A/dm², (c) 2 A/dm², (d) 2.8 A/dm², and (e) 6 A/dm² for 3 h.

These differences in cobalt deposit morphology may be due to the electrolyte solution with a cobalt concentration of 70 g/L exhibiting lower hydrogen evolution and faster cobalt supply and charge transfer at the cathode surface than the electrolyte solution with a cobalt concentration of 14 g/L, thereby resulting in a more porous cobalt deposit morphology at low cobalt concentrations.

The SEM micrograph of the cobalt deposit morphology presented in Figure 4 shows that flat and compact cobalt deposits were formed during the electrowinning of cobalt from electrolyte solutions with a cobalt concentration of 70 g/L at an applied current density of 0.8 A/dm². The shape of the cobalt particles tended to become spherical and enlarged when the current density was increased from 0.8 to 6 A/dm². The morphology of the cobalt deposits formed at low current densities was compact and uniform, but it became nonhomogeneous at high current densities. The increase in the current density stimulated hydrogen gas evolution at the cathode surface, which inhibited the cobalt deposition process and created nonhomogeneous cobalt deposits.

3.2. Effect of the cobalt (II) concentration on the current efficiency and cobalt morphology

The effect of the cobalt concentration on the current efficiency of the cobalt electrowinning process was investigated in the cobalt chloride electrolyte solutions with cobalt concentrations of 14–70 g/L at a temperature of 60 °C, pH 1.5, and different current densities ranging from 0.8 to 8 A/dm² for 3 hours.

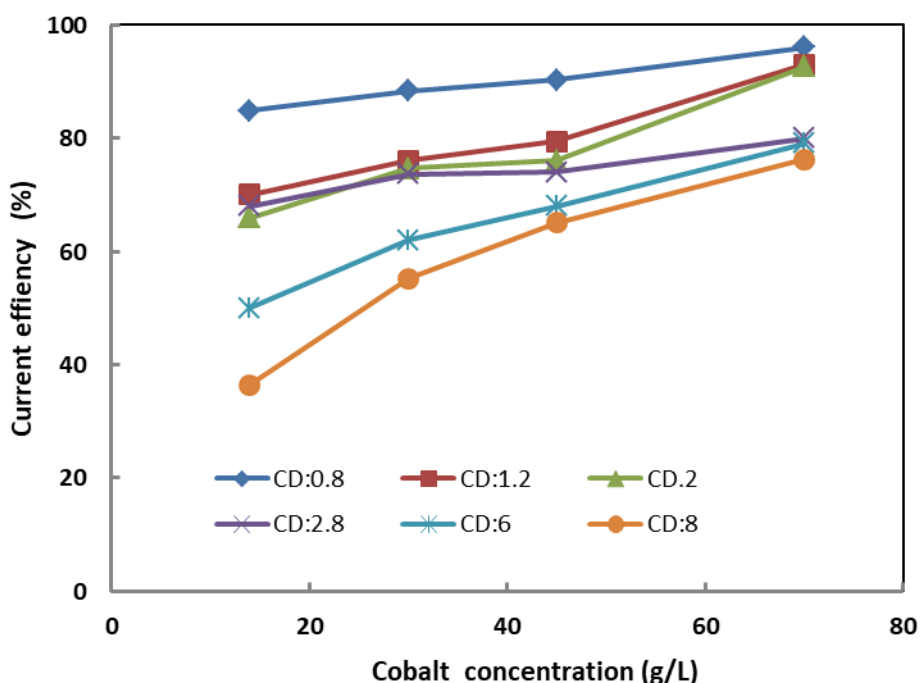


Figure 5. Effect of the cobalt concentration on the current efficiency at temperature of 60 °C, pH 1.5, and current densities of 0.8–8 A/dm² for 3 h.

The experimental results in Figure 5 demonstrate that increasing the cobalt concentration in the electrolyte solutions from 14 to 70 g/L increased the current efficiency because a high cobalt concentration in electrolyte solutions causes an increase in cobalt supply and charge transfer at the cathode surface[49] as well as a more noble reduction potential for cobalt, which in turn creates a high current efficiency[35]. Another researcher discovered a similar trend during the electrowinning of cobalt from cobalt sulfate solutions, demonstrating that current efficiency increases as the cobalt concentration increases owing to the abundant availability of cobalt ions at high concentrations[52].

The experimental results shown in Figure 5 are supported by the SEM micrographs of the cobalt deposit morphology in Figures 6 and 7, which depict the morphology of cobalt deposits formed during the electrowinning of cobalt from cobalt chloride electrolyte solutions with cobalt concentrations of 14, 30, and 70 g/L at a temperature of 60 °C, pH 1.5, and current densities of 0.8 A/dm² and 2 A/dm² for 3 hours.

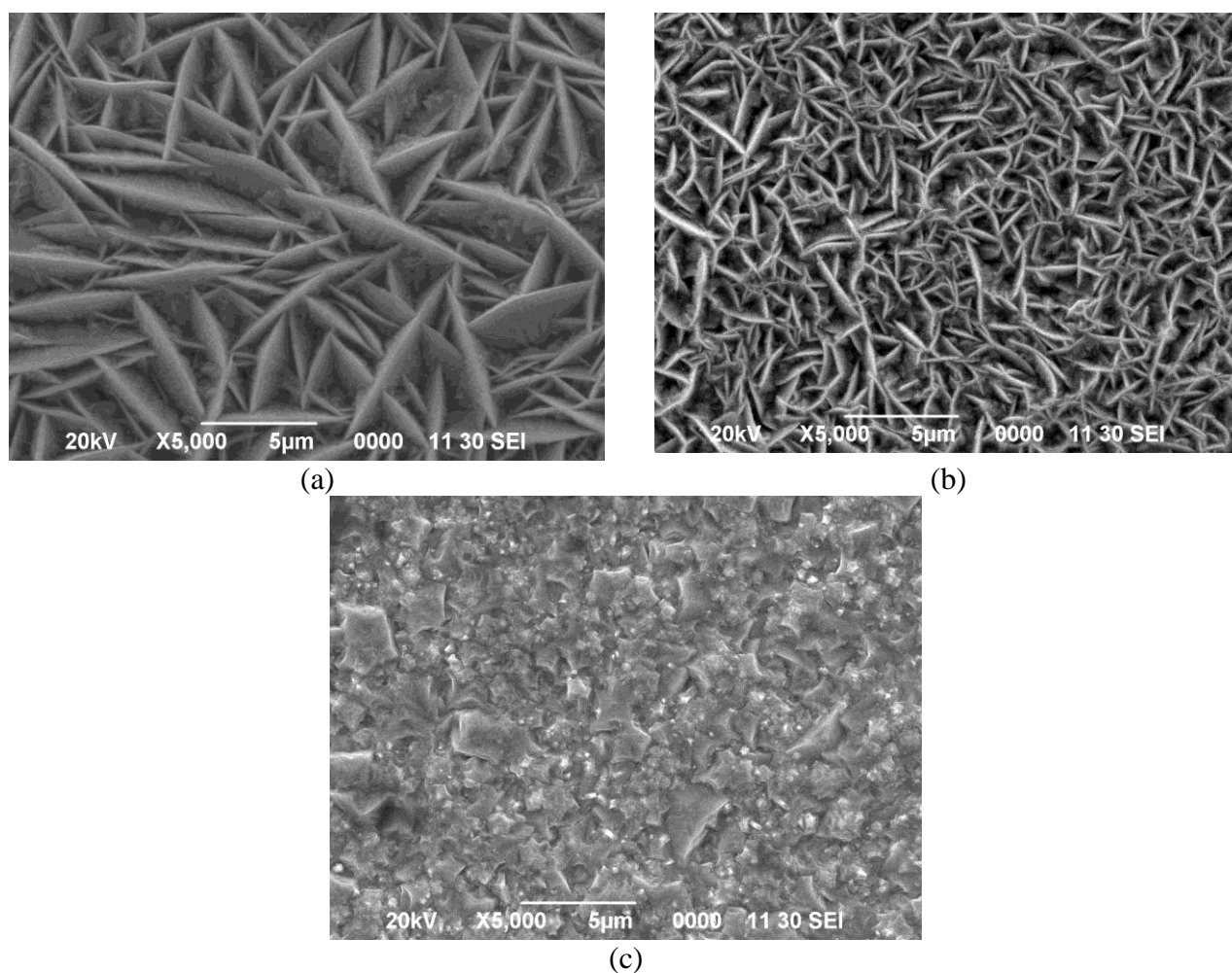


Figure 6. SEM micrograph of the cobalt deposit morphology formed during cobalt electrowinning at a temperature of 60 °C, pH 1.5, a current density of 0.8 A/dm² and cobalt concentrations of (a) 14 g/L, (b) 30 g/L, and (c) 70 g/L for 3 h.

The cobalt deposits formed in the electrolyte solutions with low cobalt concentrations were less compact and more porous than those formed in the electrolyte solutions with high cobalt concentrations. This high porosity may be due to the formation of hydrogen gas at the cathode surface, which inhibited the growth of cobalt grains. The formation of hydrogen gas consumed energy and reduced the current efficiency.

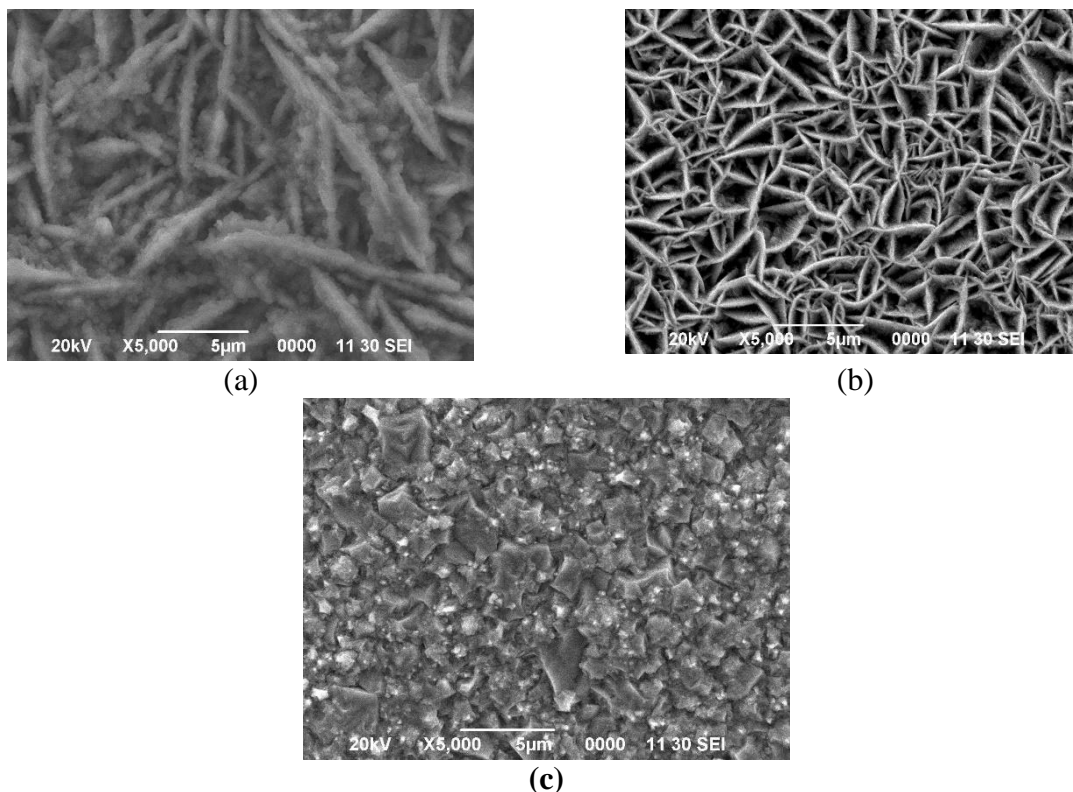


Figure 7. SEM micrograph of the cobalt deposit morphology formed during cobalt electrowinning at a temperature of 60 °C, pH 1.5, a current density of 2 A/dm² and with cobalt concentrations of (a) 14 g/L, (b) 30 g/L, and (c) 70 g/L for 3 h.

Figures 6 and 7 depict cobalt particles with a needle-like shape were formed on the cathode surface during the electrowinning of cobalt from cobalt chloride electrolyte solutions with cobalt concentrations of 14 g/L and 30 g/L. These needle-like particles created porous and incompact cobalt deposits on the cathode surface. When the cobalt concentration in the electrolyte solutions was increased from 14 to 30 g/L, the needle-like cobalt particles shrunk and created cobalt deposits with low porosities. However, when the cobalt concentration in the electrolyte solution was further increased to 70 g/L, the morphology of the cobalt deposits on the cathode surface became flat and more compact. This morphological change was due to the different mechanisms of the electrowinning process in the respective electrolyte solutions. In the electrolyte solution with low cobalt concentrations, the electrowinning process was controlled by the diffusion of ionic cobalt from the bulk electrolyte solution to the cathode surface, which resulted in a porous cobalt deposit morphology. However, in the electrolyte

solutions with high cobalt concentrations, the supply of ionic cobalt and charge transfer at the cathode surface occurred rapidly, resulting in a more compact morphology. Therefore, cobalt particles with large grain sizes were formed at low cobalt concentrations, whereas those with small grain sizes were formed at high cobalt concentrations[34].

3.3. Effect of the electrolyte solution pH on the current efficiency and cobalt morphology

The effect of the pH of the electrolyte solution on the current efficiency was investigated during the electrowinning of cobalt from cobalt chloride electrolyte solutions with cobalt concentrations of 30–70 g/L at 60 °C and an applied current density of 1.2 A/dm² for 3 hours. In this experiment, the pH of the electrolyte solutions was adjusted from 0.5 to 3. The experimental result presented in Figure 8 demonstrates that the current efficiency increased as the pH of the electrolyte solution increased from 0.5 to 2. The electrolyte solutions with a low pH decreased the current efficiency because they had higher ionic hydrogen concentrations than the electrolyte solutions with a high pH. According to equations 3 and 4, ionic hydrogen has a more positive reduction potential than ionic cobalt; therefore, it would decrease faster than ionic cobalt. The cobalt current efficiency decreased as the pH of the electrolyte solution decreased. Jiaming Lu[54] discovered a similar trend after electrowinning cobalt from a cobalt sulfate solution. Their findings indicate that an increase in pH increases the current efficiency.

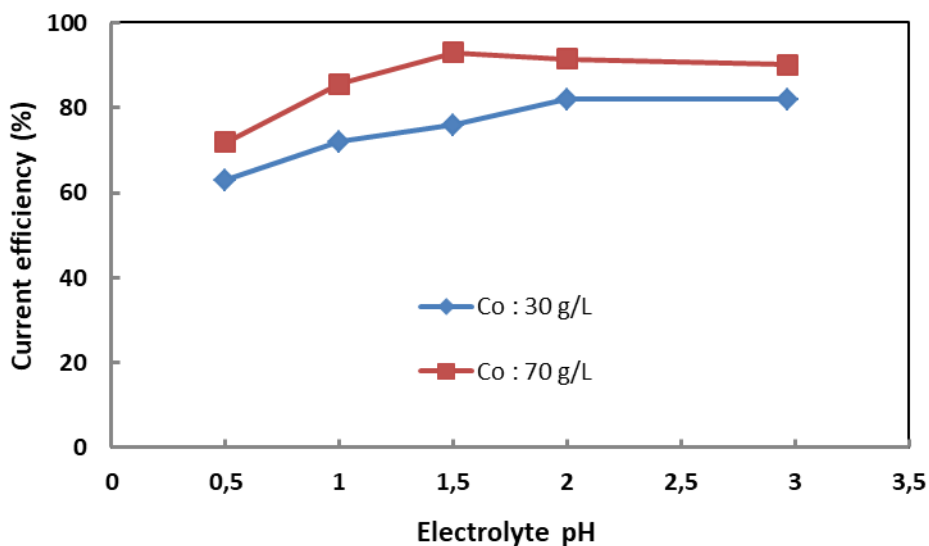


Figure 8. Effect of electrolyte pH on the current efficiency in cobalt chloride electrolyte solutions with cobalt concentrations of 30–70 g/L at 60 °C and a current density of 1.2 A/dm² for 3 h.



The experimental results depicted in Figure 8 support the SEM observations of the cobalt deposit morphology in Figures 9 and 10, which depict the morphology of the cobalt deposits formed during the electrowinning of cobalt from the cobalt chloride solutions with cobalt concentrations of 30 and 70 g/L at different pHs, a temperature of 60 °C, and an applied current density of 1.2 A/dm² for 3 hours. These Figures show that the morphology of the cobalt deposits formed at a low pH was more porous than that formed at a high pH because hydrogen evolution is higher in solutions with a low pH than in solutions with a high pH. The continuous release of hydrogen gas at the cathode surface caused the hydrogen adsorbed on the cathode surface to inhibit the growth of cobalt grains[50] and generate porous products during electrowinning[46].

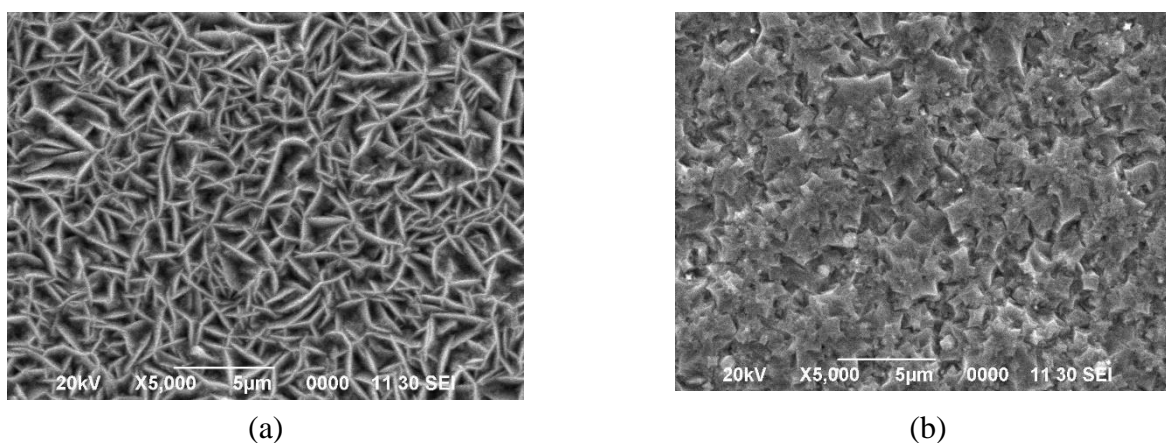


Figure 9. SEM micrograph of the cobalt deposit morphology formed during the electrowinning of cobalt from cobalt chloride solutions with a cobalt concentration of 30 g/L at temperature of 60 °C, current density of 1.2 A/dm², (a) pH 1.5 and (b) pH 2 for 3 h.

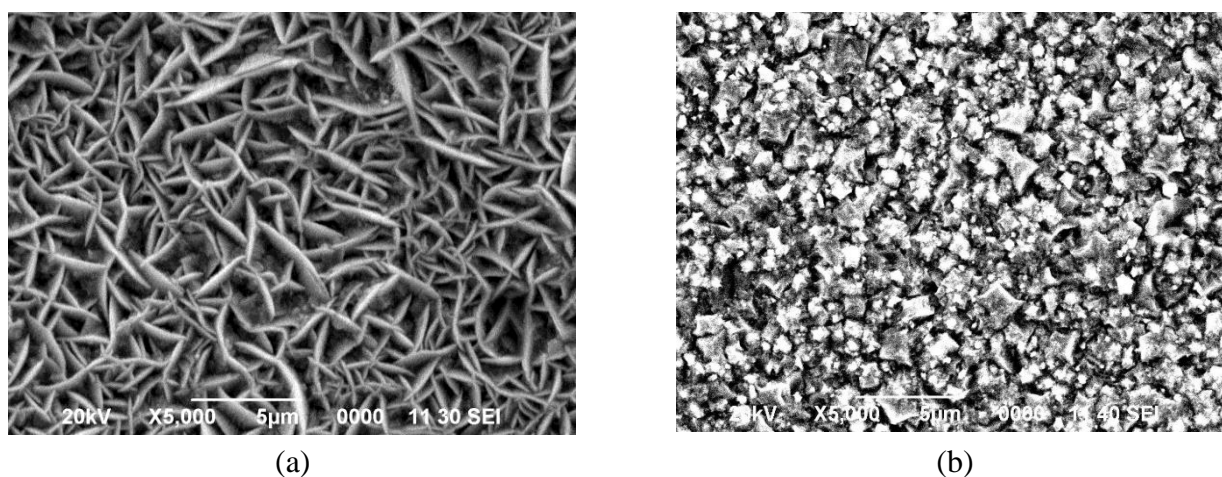


Figure 10. SEM micrograph of the cobalt deposit morphology formed during the electrowinning of cobalt from cobalt chloride solutions with a cobalt concentration of 70 g/L at temperature of 60 °C, current density of 1.2 A/dm², (a) pH 2 and (b) pH 3 for 3 h.

Figure 9 shows that the electrowinning of cobalt from the cobalt chloride solution with a cobalt concentration of 30 g/L at pH 1.5 resulted in the formation of cobalt deposits with a needle-like, porous, and incompact morphology. However, when the electrolyte pH was increased to 2, the cobalt deposit morphology changed from being needle-like to being flat, less porous, and more compact.

The change in the cobalt structure may be due to solutions with a low pH having more hydrogen evolution than solutions with a high pH during the electrowinning process[34]. Since the hydrogen gas on the cathode surface inhibited the cobalt deposition process, the morphology of the cobalt deposits became porous and incompact.

The same tendency was observed during the electrowinning of cobalt from the cobalt chloride solution with a cobalt concentration of 70 g/L, as shown in Figure 10. The morphology of the cobalt deposits formed in the electrolyte solution with a pH of 2 was more porous and less compact than those formed in the electrolyte solution with a pH of 3.

3.4. Effect of temperature on the current efficiency and cobalt morphology

The effect of the electrolyte temperature on the current efficiency was investigated during the electrowinning of cobalt from cobalt chloride solutions with cobalt concentrations of 30–70 g/L and electrolyte pH of 2 at temperatures of 30 °C–60 °C using an applied current density of 1.2 A/dm² for 3 hours. The experimental results are depicted in Figure 11. They demonstrate that the current efficiency increased from 86% to 92% when the electrolyte temperature was increased from 30 °C to 60 °C during the electrowinning of cobalt from electrolyte solutions with cobalt concentrations of 70 g/L. Previous studies[51][52] have also demonstrated that an increase in the electrolyte temperature may increase the ionic mobility and electrolyte conductivity, which may increase the current efficiency. The experimental results for the electrolyte solution with a cobalt concentration of 70 g/L (Figure 11) are supported by the SEM micrograph data depicted in Figure 12, which demonstrates that the cobalt deposit formed in the solution with a cobalt concentration of 70 g/L and at a temperature of 60 °C had more compact morphology than that formed at 30 °C. This result indicates that hydrogen gas evolution at 30 °C was significantly higher than that at 60 °C owing to ionic mobility and electrolyte conductivity at 60 °C higher than at 30 °C, which resulted in the current efficiency being higher at 60 °C than at 30 °C.

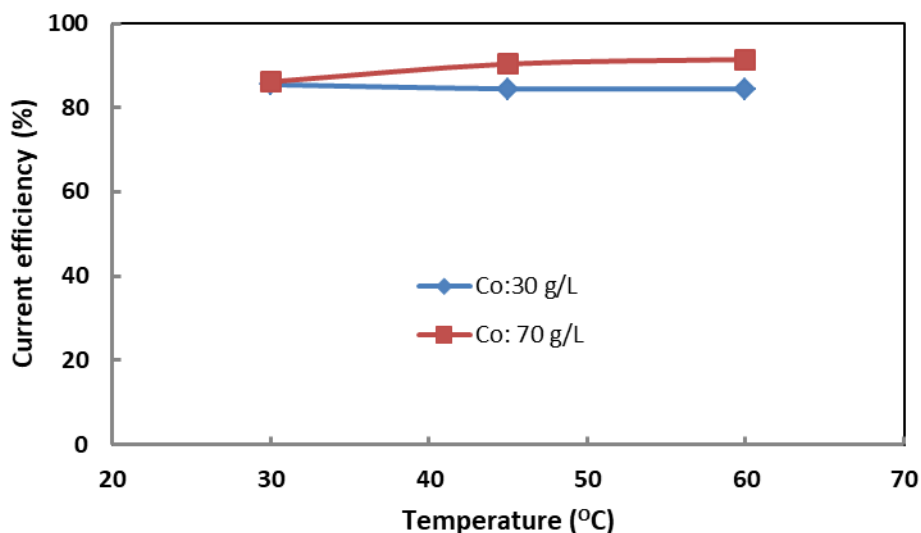


Figure 11. Effect of the electrolyte temperature on the current efficiency at a current density of 1.2 A/dm², cobalt concentrations of 30–70 g/L, pH 2, and temperatures of 30–60 °C for 3 h.

Figure 11 also depicts the experimental results for the electrowinning of cobalt from cobalt chloride solutions with a cobalt concentration of 30 g/L. The current efficiency slightly decreased when the electrolyte temperature was increased from 30 °C to 60 °C. This result is in good agreement with the SEM observations of the cobalt deposit microstructure at the cathode surface presented in Figure 13, which shows that the cobalt deposits formed at 60 °C were more porous than those formed at 30 °C. This high porosity may be due to the hydrogen evolution at 60 °C being significantly higher than that at 30 °C. Therefore, the increase in the electrolyte temperature from 30 °C to 60 °C slightly decreased the current efficiency.

When the cobalt electrowinning experimental results for the two electrolyte solutions (in Figure 11) were compared, a difference in the mechanism of the cobalt electrowinning process was discovered. For the electrolyte solution with a cobalt concentration of 70 g/L, increasing the electrolyte temperature from 30 °C to 60 °C increased the current efficiency. However, for the electrolyte solution with a cobalt concentration of 30 g/L, increasing the electrolyte temperature from 30 °C to 60 °C decreased the current efficiency. The difference in the current efficiency may be due to changes in the mechanism of the cobalt electrowinning process. The supply of ionic cobalt and the charge transfer process on the cathode surface occurred rapidly in the electrolyte solution with a cobalt concentration of 70 g/L. Conversely, the cobalt electrowinning process in the electrolyte solution with a cobalt concentration of 30 g/L was controlled by the transfer of ionic cobalt from the bulk solution to the cathode surface, which resulted in ionic cobalt deficiency at the Nernst layer, increased the hydrogen evolution, created more porous cobalt deposit at the cathode surface, and decreased the current efficiency.

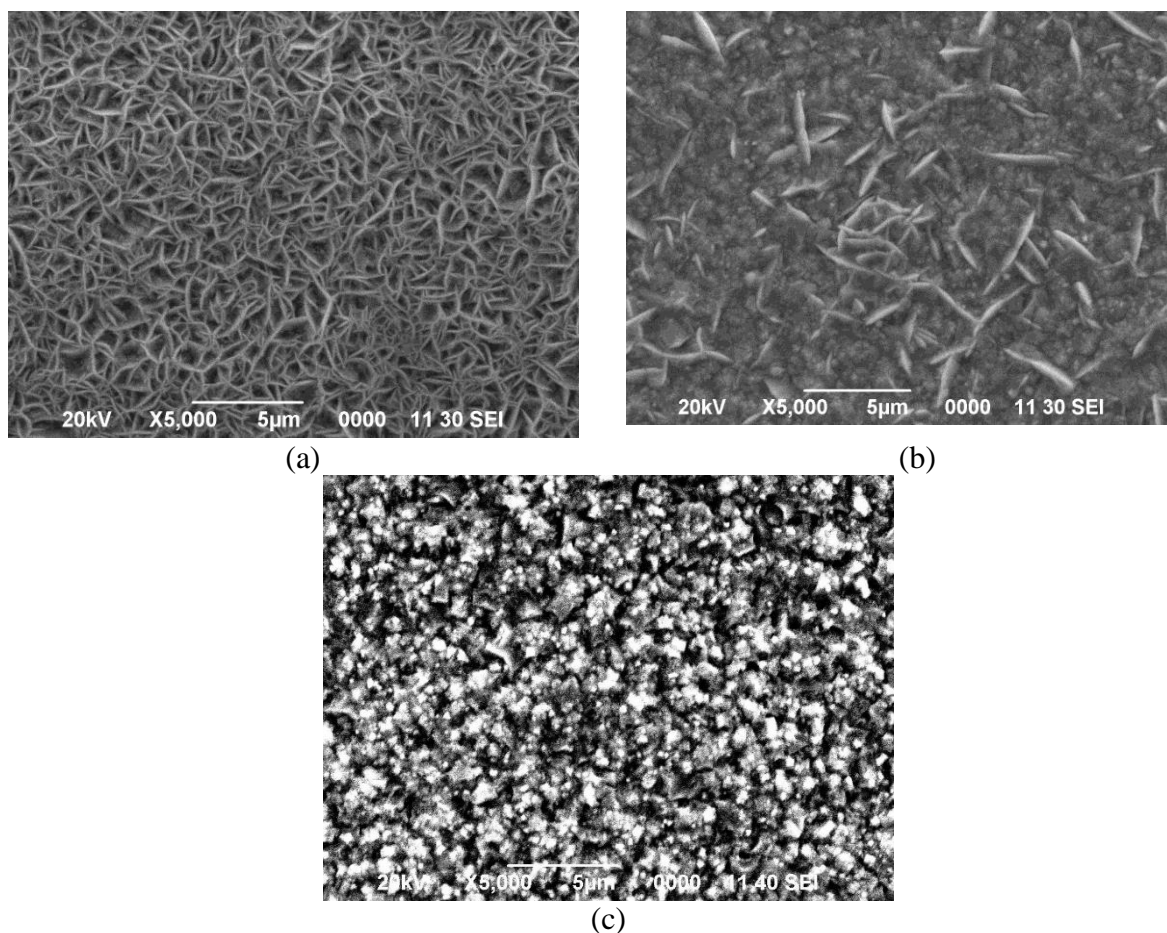


Figure 12. SEM micrograph of the cobalt deposit morphology formed during the electrowinning of cobalt from the cobalt chloride solutions with a cobalt concentration of 70 g/L, at pH 2, current density of 1.2 A/dm², and at different temperatures for 3 h: (a) 30 °C, (b) 45 °C, and (c) 60 °C.

SEM micrograph data in Figures 12 and 13 show the shape and size of the cobalt particles deposit are different depending on electrolyte temperature and cobalt concentration in solution. Figure 12 shows the small needle-like morphology of the cobalt particle deposits that were formed on the cathode surface during the electrowinning of cobalt from the cobalt chloride solution with a cobalt concentration of 70 g/L and at a temperature of 30 °C. However, the morphology of the cobalt particle deposits changed from a small needle-like particle shape to a combination of large needle-like and round particle shapes at a temperature of 45 °C, whereas the morphology of the cobalt particle deposits tended to become circular and more compact at a temperature of 60 °C.

Figure 13 shows that both small needle-shaped and oval-shaped cobalt particle deposits were formed in the cobalt chloride solutions with a cobalt concentration of 30 g/L and at a temperature of 30 °C. However, the needle-like particle shape of the cobalt deposits became larger at 45 °C, whereas the needle-like particle shape of the cobalt deposit became more porous at a temperature of 60 °C. Similar trends were found during the electrodeposition of cobalt from chloride solutions[49]. These trends demonstrated that the particles of the electrodeposits enlarged owing to a decrease in the viscosity of the electrolyte, an increase in the charge transfer rate, and an increase in the nucleus growth rate at high temperatures.

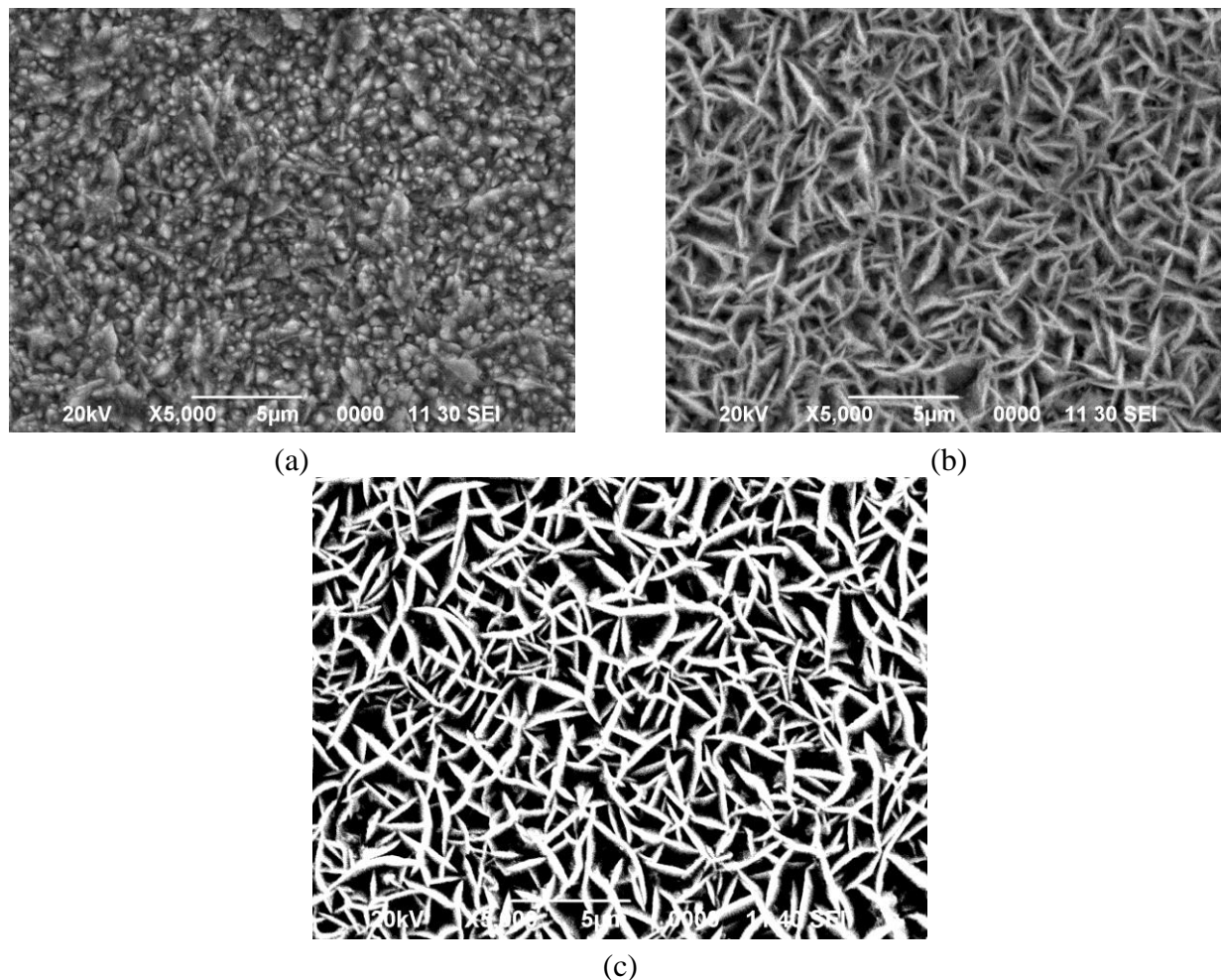


Figure 13. SEM micrograph of the cobalt deposit morphology formed during the electrowinning of cobalt from cobalt chloride solutions with a cobalt concentration of 30 g/L, at pH 2, current density of 1.2 A/dm², and at different temperatures for 3 h: (a) 30 °C, (b) 45 °C, and (c) 60 °C.

4. CONCLUSION

Cobalt chloride solutions with cobalt concentrations of 14–70 g/L were used to conduct a cobalt electrowinning experiment in order to investigate the effect of technological parameters such as current density, temperature, cobalt concentration, and electrolyte solution pH on both the current efficiency and the morphology of the cobalt deposits formed on the cathode surface. The experimental results revealed that the current efficiency and the morphology of the formed cobalt deposits were affected by the technological parameters such as the current density, temperature, cobalt concentration, and pH of the electrolyte solutions.

As the electrowinning current density increased from 0.8 to 8 A/dm², the current efficiency decreased, and a more porous and nonuniform cobalt morphology was formed because hydrogen formation was higher at a high current density than at a low current density. This hydrogen formation consumed energy, and the random formation of hydrogen gas on the electrode surface caused the surface

available for cobalt deposition to become nonhomogeneous, leading to a more porous and nonuniform cobalt deposit morphology.

When the cobalt concentration in the electrolyte solution was increased from 14 to 70 g/L, the cobalt supply and charge transfer at the cathode surface increased, and the current efficiency of the cobalt electrowinning process increased. The cobalt deposits formed at the cathode surface in the electrolyte solutions with high cobalt concentrations had a more compact morphology, whereas those formed in the electrolyte solutions with low cobalt concentrations had a large particle size and tended to become porous and incompact owing to the formation of hydrogen gas.

When the electrolyte solution pH was increased from 0.5 to 2, the formation of hydrogen gas on the cathode surface decreased, and the current efficiency of the cobalt electrowinning process increased. Therefore, the morphology of the cobalt deposit formed in the electrolyte solution with a high pH tended to become more compact than that formed in the low-pH electrolyte solutions.

When the electrowinning temperature was increased from 30 °C to 60 °C, the electrolyte conductivity and current exchange on the cathode surface increased, and this consequently increased the formation of cobalt deposits on the cathode surface as well as the current efficiency of the cobalt electrowinning process.

ACKNOWLEDGMENTS

The authors wish to acknowledge the National Innovation Research Agency, Indonesia, for funding the research activity. We also acknowledge Mrs. Rahmanisa and Mr. Adi Noor Said for their assistance in material analysis by scanning electron microscopy.

References

1. F. J. Anaissi, D. F. L. Horsth, J. Dalastra, J. O. Primo, K. W. Borth, M. L. M. Rocha and N. Balaba, *J. Braz. Chem. Soc.*, 31 (2020) 2265.
2. A. Campanile, B. Liguori, O. Marino, G. Cavaliere, V. L. De Bartolomeis and D. Caputo, *Sci. Rep.*, 10 (2020) 10147.
3. C. M. Silva, M. C. Da Silva, P. K. Rohatgi and R. A. Renzetti, *Brazilian J. Dev.*, 8 (2022) 9723.
4. X. Sun, H. Hao, Z. Liu, F. Zhao and J. Song, *Resour. Conserv. Recycl.*, 149 (2019) 45.
5. A. C. Ghogia, A. Nzihou, P. Serp, K. Soulantica and D. P. Minh, *Appl. Catal. A: Gen.*, 609 (2020) 117906.
6. B. Tian, S. Mao, F. Guo, J. Bai, R. Shu, L. Qian and Q. Liu, *Energy*, 242 (2022) 122970.
7. M. Chandrashekar and K. V. S. Prasad, *Mater. Today Proc.*, 5 (2018) 7678.
8. J. M. Costa, M. B. Porto, R. J. Amancio and A. F. D Neto, *Surf. Interfaces*, 20 (2020) 100626.
9. H. A. Zaman, S. Sharif, D. W. Kim, M. H. Idris, M. A. Suhaimi and Z. Tumurkhuyag, *Procedia Manuf.*, 11 (2017) 563.
10. C. Demminger, C. Klose and H. J. Maier, *Procedia Technol.*, 26 (2016) 35.
11. E. White, E. Rinko, T. Prost, T. Horn, C. Ledford, C. Rock and I. Anderson, *Appl. Sci.* 9 (2019) 4843
12. X. Zhou, A. Huang, B. Cui and J. W. Sutherland, *Procedia CIRP*, 98 (2021) 127.
13. G. Bailey, M. Orefice, B. Sprecher, M. A. R. Onal, E. Herraiz, W. Dewulf and K. V. Acker, *J. Clean. Prod.*, 286 (2021) 125294.
14. A. Aherwar, A. K. Singh and A. Patnaik, *Trends Biomater. Artif. Organs*, 30 (2016) 50.
15. K. Kulcsár and J. Kónya, *Acta Mater. Transilv.*, 1 (2018) 97.
16. G. Herranz, C. Berges, J. A. Naranjo, C. García and I. Garrido, *J. Mech. Behav. Biomed. Mater.*, 105 (2020) 103706

17. A. Shokrani, V. Dhokia and S. T. Newman, *Procedia CIRP*, 46 (2016) 404.
18. G. Manivasagam, D. Dhinasekaran and A. Rajamanickam, *Recent Patents Corros. Sci.*, 2 (2010) 40.
19. G. S. Seck, E. Hache and C. Barnet, *Resour. Policy*, 75 (2022) 102516.
20. R. V. Kumar and A. P. Khandale, *Renew. Sustain. Energy Rev.*, 156 (2022) 111985.
21. E. Peek, T. Åkre and E. Asselin, *JOM*, 61 (2009) 43.
22. F. K. Crundwell, N. B. du Preez and B. D. H. Knights, *Miner. Eng.*, 156 (2020) 106450.
23. P. A. Dias, D. Blagoeva, C. Pavel and N. Arvanitidis, Cobalt: demand-supply balances in the transition to electric mobility, *Publications Office of the European Union*, (2018) Luxembourg.
24. Q. Dehaine, L. T. Tijsseling, H. J. Glass, T. Törmänen and A. R. Butcher, *Miner. Eng.*, 160 (2021) 106656.
25. N. Mulaudzi, M. H. Kotze, Direct cobalt electrowinning as an alternative to intermediate cobalt mixed hydroxide product, *Seventh Southern African Base Metals Conference*, Mpumalanga, South Africa, (2013) 209.
26. K. G. Fisher, Cobalt Processing Developments, *6th Southern African Base Metals Conference*, Phalaborwa, South Africa, (2011) 237.
27. K. A. Karimov, A. V. Kritskii, L. G. Elfimova and S. S. Naboichenko, *Metallurgist*, 61 (2017) 238.
28. Y. Huang, Z. Zhang, Y. Cao, G. Han, W. Peng, X. Zhu, T. A. Zhang and Z. Dou, *Hydrometallurgy*, 193 (2020) 105327.
29. S. S. Afolabi, M. O. Zakariyah, M. H. Abedi and W. Shafik, *J. Indian Chem. Soc.*, 98 (2021) 100179.
30. J. Cheng, T. Lu, X. Wu, H. Zhang, C. Zhang, C. A. Peng and S. Huang, *RSC Adv.*, 9 (2019) 22729.
31. R. Subagja, *IOP Conf. Ser. Mater. Sci. Eng.*, 285 (2018) 012001.
32. M. H. Morcali, L. T. Khajavi, S. Aktas and D. B. Dreisinger, *Hydrometallurgy*, 185 (2019) 257.
33. A. D. Dalvi, W. G. Bacon and R. C. Osborne, The Past and the Future of Nickel Laterites, *PDAC 2004 Int. Conv.*, Charlotte North Carolina, USA, (2004) 1.
34. S. Banbur-Pawłowska, K. Mech, R. Kowalik and P. Zabinski, *Appl. Surf. Sci.*, 388 (2016) 805.
35. S. Mahdavi and S. R. Allahkaram, *Trans. Nonferrous Met. Soc. China*, 28 (2018) 2017.
36. Z. Wang, A. T. Aji, B. P. Wilson, S. Jørstad, M. Møll and M. Lundström, *Metals*, 11 (2021) 1824.
37. K. G. Mishra, P. Singh and D. M. Muir, *Hydrometallurgy*, 65 (2002) 97.
38. A. Mirza, M. Burr, T. Ellis, D. Evans, D. Kakengela, L. Webb, J. Gagnon, F. Leclercq and A. Johnston, *J. South. African Inst. Min. Metall.*, 116 (2016) 533.
39. I. Korolev, K. Yliniemi, M. Lindgren, L. Carpén and M. Lundström, *Metall. Mater. Trans. B*, 52B (2021) 3107.
40. W. Zhang, E. Ghali and G. Houlachi, *Hydrometallurgy*, 169 (2017) 456.
41. M. Nusheh and H. Yoozbashizadeh, *Iranian J. Mater. Sci. Eng.*, 7 (2010) 45.
42. Y. Yu, Z. Song, H. Ge, G. Wei and L. Jiang, *Int. J. Electrochem. Sci.*, 10 (2015) 4812.
43. B. M. Trivedi and G. Prabakaran, *RREC.*, 5 (2014) 92.
44. P. Patnaik, S. K. Padhy, B. C. Tripathy, I. N. Bhattacharya and R. K. Paramguru, *Trans. Nonferrous Met. Soc. China*, 25 (2015) 2047.
45. S. C. Kwak, B. K. Kim, D. I. Kim and Y. W. Cho, *Korean J. Met. Mater.*, 55 (2017) 768.
46. Q. Song, Y. Zhao, C. Wang, H. Xie, H. Yin and Z. Ning, *Hydrometallurgy*, 189 (2019) 105111.
47. P. C. Hayes, *Process Selection in Extractive Metallurgy*, Hayes Publishing, (1985) Brisbane, Australia.
48. N. Ramos-Lora, L. H. Mendoza-Huizar and C. H. Rios Reyes, *J. Chil. Chem. Soc.*, 56 (2011) 631.
49. X. Cao, L. Xu, Y. Shi, Y. Wang and X. Xue, *Electrochim. Acta*, 295 (2019) 550.
50. E. H. Moradi, K. Jafarzadeh, S. Borji and H. Abbaszadeh, *Miner. Eng.*, 77 (2015) 10.
51. W. Zhang, X. Chen, Y. Wang, L. Wu and Y. Hu, *ACS Omega*, 5 (2020) 22465.

52. I. G. Sharma, P. Alex, A. C. Bidaye and A. K. Suri, *Hydrometallurgy*, 80 (2005) 132.
53. J. H. Huang, C. Kargl-Simard and A. M. Alfantazi, *Can. Metall. Quart.*, 43 (2004) 163.
54. J. Lu, D. Dreisinger and T. Glück, *Hydrometallurgy*, 178 (2018) 19.

© 2022 The Authors. Published by ESG (www.electrochemsci.org). This article is an open access article distributed under the terms and conditions of the Creative Commons Attribution license (<http://creativecommons.org/licenses/by/4.0/>).